Correlation of Type I ELM Energy losses with pedestal plasma characteristics and global discharge parameters in JET ELMy H-modes

A Loarte [1], G Saibene [1], R Sartori [1], M Becoulet [2], P J Lomas [3], S. Ali-Arshad [3], B. Alper [3],

M Beurskens [4], M Kempenaars [4], R Koslowski [5], C P Pérez [5], A Kallenbach [6], W Suttrop [6]

and contributors to the EFDA-JET workprogramme

[1]*EFDA Close Support Unit (Garching), 2 Boltzmannstrasse, Garching, Germany*
[2]*Association Euratom-CEA, Cadarache, F-13108 St. Paul-lez-Durance, France*
[3]*Euratom/UKAEA Association, Culham Science Centre, Abingdon, OX14 3DB, UK*
[4]*Association EURATOM-FOM, FOM Rijnhuizen, P.O. Box 1207, 3430 BE, Netherlands*
[5]*Forschungszentrum Jülich GmbH, Institut f Plasmaphysik, EURATOM Association,*
Trilateral Euregio Cluster, 52425 Jülich, Germany
[6]*Association Euratom-IPP, MPI fur Plasmaphysik, 2 Boltzmannstrasse, Garching, Germany*

1. Introduction.

The Type I ELMy H-mode regime is the reference regime for inductive operation of ITER [1]. A major drawback of this regime is the periodic large power loads on plasma facing components associated with Type I ELMs that may lead to unacceptable divertor target lifetime reduction when extrapolated to next step devices [2]. Type I ELM energy losses in JET are well correlated with the pedestal plasma parameters [3], but there is a considerable scatter in this dependence, indicating that other additional factors contribute in a significant way to the mechanisms determining the Type I ELM energy loss from the main plasma. In order to determine some of these additional factors, a wide range of experiments has been carried out at JET, including scans of additional heating power (6 – 18 MW), deuterium fuelling rates ($0 - 10^{23}$ s^{-1}), plasma current (1.1 – 3 MA), q_{95} (2.8 – 5.2) and plasma shaping (δ = 0.20 – 0.43). In these experiments the ELM energy loss, pedestal parameters and gradients (only for a set of plasma configurations and plasma currents [4]) and ELM crash characteristics (ELM energy loss, width of the ELM affected volume, duration of the ELM-crash from MHD activity, etc.) have been determined. Fig. 1 shows the values of pedestal temperature and density before the Type I or III ELMs for the discharges in this study.

2. Global Pedestal and ELM Characteristics.

Type I ELMs at JET occur when the values of density and temperature at the H-mode pedestal (n_{ped}, T_{ped}) exceed a certain limit, which depends on discharge parameters. The scatter around the average value of this limit for n_{ped} and T_{ped} is very small (typically less than 20%) for a large range of main plasma parameters (i.e., average limit values). Despite this reproducibility of the pedestal plasma parameters before the ELM, the collapse of the edge pedestal temperature ($\Delta T_{e,ped}$) and density ($\Delta n_{e,ped}$) and the associated ELM energy loss (ΔW_{ELM}) show a much larger variation as shown in Fig. 2 for ΔW_{ELM}, illustrating the "natural" ELM variability caused by the variations in the ELM collapse for similar pre-ELM pedestal plasma parameters in a large range of discharges. In this paper we will study the

correlation of the average values for Type I ELM energy and particle losses with plasma parameters.

The Type I ELM frequency at JET, f_{ELM}, scales approximately with P_{INP}/I_p^2 and, for given P_{INP}/I_p^2, it increases with the level of gas puffing (or n_{ped}) in the absence of Type I/II mixed regimes [5], which for the discharges considered in this study were only found in the high triangularity configuration ($\delta = 0.43$) HT3 at currents of 2.5MA. I_p, q_{95} scans have been performed in this configuration at 2MA ($q_{95} = 3.6 - 5.2$) and 2.5MA ($q_{95} = 3.6 - 4.6$). In these scans it has been observed that $f_{ELM} \sim q_{95}^{\alpha}$, with $3<\alpha<4$, at similar normalised pedestal densities $n_{ped}/n_{Greenwald}$. Measurements of pedestal plasma gradients in the discharges at 2MA [4] indicate that for similar $n_{ped}/n_{Greenwald}$ the pedestal pressure gradients are similar at both q_{95} indicating that the increased f_{ELM} is probably linked to changes in edge transport with increasing q_{95} [6]. For a range of plasma conditions, the average power flux ($f_{ELM} \times \Delta W_{ELM}$) carried by the Type I ELMs in JET reaches $\sim 50\%$ of P_{INPUT} and, hence, it is a dominant term in the total power balance.

3. Type I ELM Energy and Particle Losses.

With increasing $n_{ped}/n_{Greenwald}$ the normalised Type I ELM energy losses ($\Delta W_{ELM}/W_{ped}$) decrease. This is mostly due to the decrease of ELM conductive losses (as estimated by relative drop of the pedestal plasma temperature at the ELM ($\Delta T_{ELM}/T_{ped}$)), while ELM convective losses (as estimated by relative drop of the pedestal plasma density at the ELM ($\Delta n_{ELM}/n_{ped}$)) remain approximately constant, as shown in Figs. 3 and 4. For similar $n_{ped}/n_{Greenwald}$, the higher I_p discharges have large values of T_{ped} and $\Delta T_{ELM}/T_{ped}$, and consequently larger $\Delta W_{ELM}/W_{ped}$. Discharges with higher levels of additional heating show smaller $\Delta n_{ELM}/n_{ped}$, $\Delta T_{ELM}/T_{ped}$ and $\Delta W_{ELM}/W_{ped}$, particularly at low $n_{ped}/n_{Greenwald}$. Increasing q_{95} leads to a substantial reduction of $\Delta T_{ELM}/T_{ped}$ ($\sim$ a factor > 2) but not of $\Delta n_{ELM}/n_{ped}$, indicating that increasing connection lengths at the plasma edge lead to a reduction of conductive losses during ELMs but not of convective losses. In the transition from Type I to Type III ELMs both $\Delta n_{ELM}/n_{ped}$, $\Delta T_{ELM}/T_{ped}$ show a sharp, decrease in agreement with the marked reduction of ΔW_{ELM} at this transition.

Because of the T_{ped} influence on the ELM conductive energy losses discussed above, $\Delta W_{ELM}/W_{ped}$ is better correlated with ν^*_{ped} (see Fig. 5) than with $n_{ped}/n_{Greenwald}$ (see Fig. 6) for JET Type I ELMs. Despite the good overall correlation shown in Fig. 5 some deviations from this correlation are found, as expected from the arguments above, for discharges with large P_{inp}. These discharge have smaller $\Delta W_{ELM}/W_{ped}$ for similar values of ν^*_{ped} than discharges with lower P_{inp} (this is clearer at lower ν^*_{ped}). Discharges at high q_{95} indeed have very small ELM energy losses $\Delta W_{ELM}/W_{ped}$. Unfortunately, for the conditions explored so far in JET, ΔW_{ELM} is under the detection limit of the diamagnetic loop and it is not possible to quantify the deviation from the collisionality correlation for such discharges.

4. ELM Affected Volume and Timescale of ELM collapse.

In order to determine possible factors besides ν^*_{ped} that may account for the scatter in Fig. 5, the volume of the plasma over which the ELM collapse occurs has been characterised at JET

by high time resolution ECE measurements of the plasma temperature before and after the ELM. Fig. 7 shows the normalised radius of the innermost point reached by the temperature collapse caused by the ELM (1-ρ_{ELM}) for a range of plasma conditions. The new experiments are in good agreement with previous JET results [3] with discharges at lower triangularities and higher q_{95} having the smaller ELM affected volumes and with the ELM affected volume being weakly dependent on plasma density. However, there is no direct correlation between this ELM affected volume and the ELM energy loss that can explain the scatter in Fig. 5. Smaller $\Delta W_{ELM}/W_{ped}$ is associated with smaller $\Delta T_{ELM}/T_{ped}$ for given plasma global parameters, with the temperature change caused by the ELM being smaller in magnitude but occurring over the same volume of the plasma. Hence, the factors that determine the scatter in Fig. 5 remain to be identified.

Finally, the duration of the ELM collapse has been characterised at JET by using the characteristic time of the pedestal plasma soft X-ray emission collapse following an ELM and by the duration of the period of broadband MHD activity associated with the Type I ELMs. Both measurements indicate that the ELM collapse time in JET is of the order of 200 – 300 μs and it is basically independent of plasma (global) and pedestal conditions, as shown in Fig. 8 (τ_{ELM} estimated from the duration of the MHD broadband activity). This indicates that the mechanism that leads to the destruction of the edge flux surfaces during an ELM is not of a Kadomtsev-type reconnection but probably of an explosive-type [7] but a comparison of the timescale magnitude and dependence on plasma parameters with JET experimental data remains to be done.

5. Conclusions.

A large dataset of simultaneous measurements of ELM bulk plasma losses, pedestal parameters and gradients, ELM divertor fluxes and MHD activity for a large range of I_p, q_{95}, δ and P_{inp} has been obtained at JET in density scans from Type I to Type III ELMy H-modes (reaching the H-L transition in some cases). The new results are in broad agreement with previously found trends for JET Type I ELMs. Deviations from previously observed trends of ΔW_{ELM} with ν^*_{ped} occur at high q_{95} and high P_{inp} (at lower ν^*_{ped}). These deviations are not explained by accompanying variations in ELM affected area. Further detailed analysis of the existing measurements and further experiments are needed to provide a firmer basis to extrapolate the measured ELM energy losses to ITER in a more precise way than so far done. In particular, this issue will be addressed in extensive low ν^*_{ped} experiments (high I_p + high P_{inp}) at ITER-like ν^*_{ped} values that will be carried out in the JET 2003/2004 experimental campaigns.

6. References.

[1] ITER Physics Basis, Nucl. Fusion 39 (1999) 2137.
[2] Janeschitz, G., et al., Jour. Nucl. Mat. 290-293 (2001) 1.
[3] Loarte, A., et al., Plasma Phys. Control. Fusion 44 (2002) 1815.
[4] Kempenaars, M., et al., these proceedings.
[5] Saibene, G., et al., Plasma Phys. Control. Fusion 44 (2002) 1769.
[6] Saibene, G., et al., these proceedings.
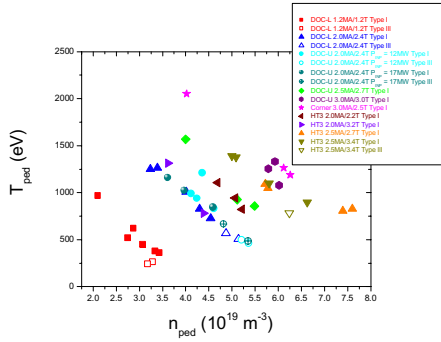[7] Cowley, S.C., et al., these proceedings.

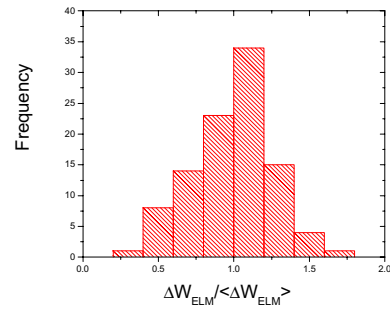*Figure 1. Pedestal plasma parameters before ELMs for the JET experiments described in this paper.*

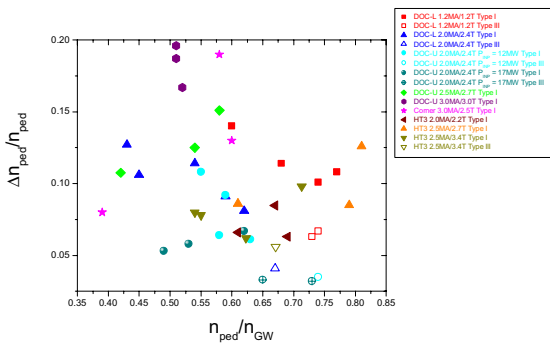*Figure 2. Histogram of the Type I ELM energy loss for a large range of plasma conditions at JET.*

Figure 3. Normalised Type I ELM pedestal density drop versus pedestal density (normalised to the Greenwald limit) for the same dataset as Fig. 1.
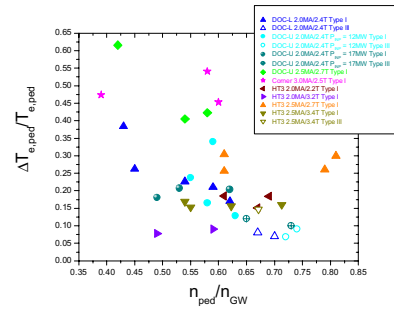

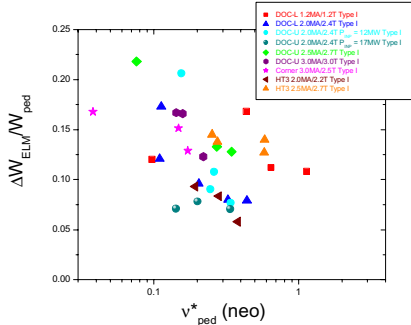*Figure 4. Normalised Type I ELM pedestal temperature drop versus pedestal density (normalised to the Greenwald limit) for the same dataset as Fig. 1.*

Figure 5. Normalised (to the pedestal energy) Type I ELM energy loss versus pedestal collisionality for the same dataset as Fig. 1.
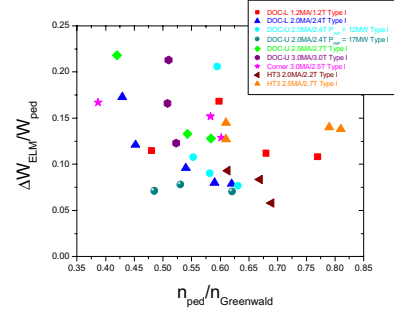

Figure 6. Normalised (to the pedestal energy) Type I ELM energy loss versus pedestal density (normalised to the Greenwald limit) for the same dataset as Fig. 1.
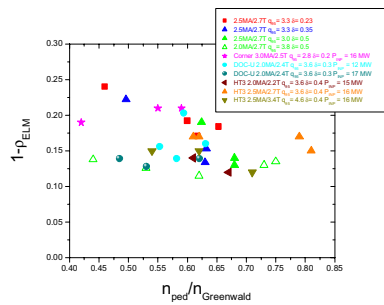

Figure 7. ELM affected radius ($1-\rho_{ELM}$) versus fuelling rate for a series of previous discharges in the JET MkII Gas Box divertor and some of the recent experiments.
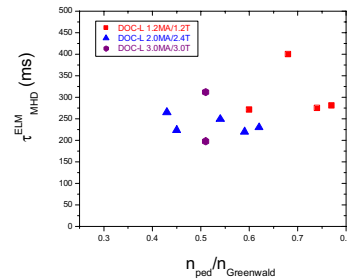

Figure 8. Duration of the ELM (from broadband MHD turbulence analysis) versus pedestal density (normalised to the Greenwald limit) for the some of the discharges in Fig. 1.